axioms

MDPI

Article

A Weighted Relational Graph Model for Emergent Superconducting-like Regimes: Gibbs Structure, Percolation, and Phase Coherence

Bianca Brumă [1], Călin Gheorghe Buzea [2,3], Diana Mirilă [4,*], Valentin Nedeff [4], Florin Nedeff [4], Maricel Agop [4], Ioan Gabriel Sandu [5] and Decebal Vasincu [6]

[1] Faculty of Physics, "Alexandru Ioan Cuza" University of Iasi, 700506 Iasi, Romania; bianca_andreea_bruma@yahoo.com
[2] National Institute of Research and Development for Technical Physics, IFT Iași, 700050 Iași, Romania; calinb2003@yahoo.com
[3] Clinical Emergency Hospital "Prof. Dr. Nicolae Oblu" Iași, 2 Ateneului Street, 700309 Iași, Romania
[4] Department of Environmental Engineering, Mechanical Engineering and Agritourism, Faculty of Engineering, "Vasile Alecsandri" University of Bacău, 600115 Bacău, Romania; vnedeff@ub.ro (V.N.); florin_nedeff@ub.ro (F.N.); m.agop@yahoo.com (M.A.)
[5] Faculty of Materials Science and Engineering, Gheorghe Asachi Technical University of Iasi, 67 Dimitrie Mangeron Blvd, 700050 Iași, Romania; ioan-gabriel.sandu@academic.tuiasi.ro
[6] Faculty of Medicine, "Grigore T. Popa" University of Medicine and Pharmacy Iași, 700115 Iași, Romania; decebal.vasincu@umfiasi.ro
* Correspondence: miriladiana@ub.ro

Abstract

We introduce a minimal relational network model in which superconducting-like behavior emerges as a collective phase of constrained connectivity and phase coherence, without assuming microscopic electrons, phonons, or material-specific interactions. The model is formulated as a concrete instantiation of a previously introduced axiomatic relational–informational framework for emergent geometry and effective spacetime, in which geometry and effective forces arise from constrained information flow rather than from a background manifold. Mathematically, this construction is realized on a finite weighted graph with binary edge-activation variables and compact vertex phase variables, sampled through a Gibbs ensemble generated by an additive informational action. The system is represented as a finite weighted graph with weighted edges encoding transport or informational costs, augmented by dynamically activated low-cost channels and compact phase degrees of freedom defined at vertices. The effective edge costs induce a weighted shortest-path metric, providing an operational notion of emergent relational geometry. Using Monte Carlo simulations on two-dimensional periodic lattices, we show that the same informational action supports three distinct emergent regimes: a normal resistive phase, a fragile low-temperature-like superconducting phase characterized by noise-sensitive coherence, and a noise-robust high-temperature-like superconducting phase in which global phase coherence persists under substantial fluctuations. These regimes are identified using purely relational observables with direct graph-theoretic and statistical-mechanical interpretation, including percolation of low-cost channels, phase correlation functions, an operational phase stiffness (helicity modulus), and a geometric diagnostic based on relational ball growth. In particular, we extract an effective geometric dimension from the scaling of low-cost accessibility balls, using a ball-growth relation of the form $\langle B(r) \rangle \sim r^{d_{eff}}$, revealing a clear monotonic hierarchy between normal, fragile superconducting, and noise-robust superconducting—like regimes. This demonstrates that superconducting-like behaviour in the present framework corresponds not only to percolation and phase alignment, but

Check for updates

Academic Editor: Giovanni Nastasi

Received: 3 March 2026
Revised: 15 April 2026
Accepted: 23 April 2026
Published: 25 April 2026

Copyright: © 2026 by the authors. Licensee MDPI, Basel, Switzerland. This article is an open access article distributed under the terms and conditions of the Creative Commons Attribution (CC BY) license.

also to a qualitative reorganization of relational geometry. Robustness is tested via finite-size comparison between 8×8, 12×12 and 16×16 lattice realizations. Within this framework, normal and superconducting-like behavior arise from the same underlying relational mechanism and differ only in the structural stability of connectivity, coherence, and geometric accessibility under fluctuations. The aim of this work is structural rather than material-specific: we do not reproduce detailed experimental phase diagrams or microscopic pairing mechanisms, but identify minimal relational conditions under which low-dissipation, phase-coherent transport can emerge as a generic organizational regime of constrained relational systems.

Keywords: relational–informational framework; emergent geometry; superconducting-like behavior; superconducting-like regimes; phase coherence; helicity modulus; phase stiffness; percolation; complex networks; statistical mechanics; XY model; Monte Carlo simulation; emergent phases; constrained information flow; finite-size scaling; geometric dimension; network phase transitions; structural organization

MSC: 05C82; 82B20; 82B26; 82B80; 37B15

1. Introduction

Superconductivity represents one of the most striking examples of macroscopic coherence in physics. Below a critical temperature T_c, electrical resistance vanishes and transport becomes governed by a collective phase extending across the entire system. In conventional superconductors, this phenomenon is successfully explained by the Bardeen–Cooper–Schrieffer (BCS) theory, where electrons form weakly bound Cooper pairs mediated by lattice vibrations, leading to a condensate with long-range phase coherence [1,2]. By contrast, high-temperature superconductivity (HTSC), discovered in layered copper-oxide materials [3], has resisted a comparably universal theoretical description despite decades of experimental and theoretical investigation [4–6].

A persistent difficulty in understanding HTSC is that many of its defining features—strong electronic correlations, reduced effective dimensionality, spatial inhomogeneity, and the prominence of collective excitations—do not fit naturally within weak-coupling or quasiparticle-based frameworks. Numerous proposals have been advanced, including resonating valence bond states [7], spin-fluctuation-mediated pairing [8], emergent gauge fields [9], and strongly correlated quantum critical scenarios [10]. While these approaches differ substantially in microscopic detail, they share a common implication: superconductivity, particularly at high temperatures, appears to be a collective organizational phenomenon rather than the straightforward consequence of a single dominant interaction.

This observation motivates a shift in perspective. Instead of asking which microscopic mechanism produces superconductivity in a given material, one may ask a more structural question: what minimal conditions are sufficient for superconductivity to emerge at all? Addressing this question requires a framework in which coherence, transport, and effective dynamics can arise without being imposed a priori.

In parallel with developments in condensed matter physics, recent work across network-based, relational, and information-theoretic approaches has explored how large-scale organization, geometry, and effective dynamics may emerge from constrained interactions rather than from a fixed background structure [11–14]. In particular, the axiomatic relational–informational framework developed in [14] proposes that physical geometry and effective forces arise from a minimal substrate consisting solely of degrees of freedom connected by admissible informational relations subject to quantifiable constraints. Within

that framework, distance is defined operationally via minimal constraint cost along relational paths, curvature arises from heterogeneity in constraint structure, and effective forces emerge as gradients of an informational action under coarse-graining. No background spacetime or predefined geometry is assumed.

The present work extends this axiomatic framework to the study of superconducting-like behavior within a relational setting. Rather than introducing electrons, phonons, or microscopic order parameters as fundamental ingredients, we ask whether superconducting behavior can emerge as a phase of constrained relational information. In this setting, transport is governed by accessibility through a network of constraints, and macroscopic behavior reflects how low-cost pathways organize statistically across the relational structure. Superconducting-like behavior is then identified operationally as a regime in which a particular transport channel becomes system-spanning and phase-coherent, allowing currents or information to propagate without accumulating effective resistance.

This relational interpretation naturally accommodates both normal conduction and superconductivity within a single conceptual scheme. A normal conducting phase corresponds to a regime in which low-cost pathways are fragmented and phase correlations are short-ranged. Within the present framework, superconducting-like behavior emerges when low-constraint connectivity percolates across the system and phase coherence becomes long-ranged. Crucially, the distinction between low-temperature and high-temperature superconductivity is reinterpreted not as a difference in fundamental mechanisms, but as a difference in the robustness of coherent relational organization against fluctuations. Low-temperature superconductors correspond to marginally stable coherence that survives only under strong noise suppression, while high-temperature superconductors correspond to regimes in which the relational structure itself strongly favors coherent, low-cost transport.

From this perspective, high-temperature-like superconducting behavior is not anomalous but structurally natural within the relational model. The same relational principles that give rise to emergent geometry and effective forces also permit the emergence of globally coherent, low-dissipation transport when constraint organization and phase stiffness are sufficiently favorable. Geometry, forces, and superconductivity thus appear as different manifestations of emergent order within constrained relational systems.

The goal of this paper is therefore foundational rather than material-specific. We do not aim to replace existing microscopic theories of superconductivity, nor to reproduce detailed experimental phase diagrams. Instead, we seek to demonstrate that superconducting-like behavior—encompassing both low-temperature-like and high-temperature-like regimes—can arise generically within a relational–informational framework consistent with the axioms introduced in [14]. By doing so, we clarify which aspects of superconducting behavior are structural and universal, and which depend on particular physical realizations.

Concretely, we show in Section 5 that by varying only a small set of relational parameters controlling cost reduction, channel activation, and phase stiffness, the same informational action gives rise to three distinct organizational regimes. These correspond to a normal resistive phase with fragmented low-cost connectivity, a low-temperature-like superconducting phase in which coherence is fragile and noise-sensitive, and a high-temperature-like superconducting phase in which a system-spanning low-cost network supports robust long-range coherence even under substantial fluctuations. In addition to connectivity and correlation-based diagnostics, we compute an operational phase stiffness (helicity modulus) and perform a finite-size comparison between 8×8, 12×12 and 16×16 lattice realizations, which together confirm that the three relational regimes differ not only in percolation properties but also in their phase rigidity and robustness to system-size enlargement.

In addition to connectivity and phase coherence, we show that the emergence of superconducting behavior is accompanied by a qualitative reorganization of relational geometry. By analyzing the growth of low-cost accessibility balls within the relational network, we extract an effective geometric dimension that increases monotonically from the normal to the fragile and noise-robust superconducting-like regimes. This demonstrates that superconducting-like behavior in the present framework corresponds not only to percolation and phase alignment, but also to an emergent extension and densification of relational geometry itself.

Although the present framework is relational and axiomatic in origin, the operational diagnostics used to identify superconducting phases are grounded in established statistical-physics traditions. In particular, the phase coherence sector is analyzed using an XY-like phase stiffness observable (helicity modulus) that measures the energetic cost of global phase twists [15–18], while the transport backbone is characterized using percolation-inspired connectivity diagnostics [19]. These tools do not impose microscopic assumptions but provide a transparent bridge between the relational formalism and the broader theory of phase transitions and collective organization. The methodology therefore situates the present model within the conceptual lineage of XY systems, phase-stiff states, and connectivity-driven critical phenomena, while preserving the axiomatic relational–informational foundation.

From a mathematical perspective, the present construction is a finite weighted graph model with mixed discrete–compact state space. Binary edge variables $p_e \in \{0, 1\}$ determine an activated low-cost subgraph, while compact vertex phases $\phi_i \in S^1$ define a phase field on the vertex set. The statistical ensemble is induced by a Gibbs weight $P_\beta(\omega) \propto e^{-\beta S(\omega)}$ associated with the informational action. The main objects studied are the weighted shortest-path metric generated by the effective edge costs, the connected-component structure of the activated subgraph, graph-distance phase correlations, an operational helicity modulus, and an effective geometric dimension extracted from ball-growth scaling. In this sense, the model lies at the interface of graph theory, percolation theory, lattice spin systems, complex networks, and mathematical physics [20–23].

The formal contribution of this work is fourfold. First, we define a minimal weighted relational graph model compatible with the previously introduced axiomatic relational–informational framework. Second, we specify a family of observables that jointly characterize connectivity, coherence, phase rigidity, and relational geometric accessibility. Third, we show numerically that the same action supports three distinct finite-size organizational regimes—normal, fragile superconducting-like, and noise-robust superconducting-like—without changing the underlying formal structure of the model. Fourth, we show that these regimes are accompanied by a monotone hierarchy in effective geometric dimension, thereby linking coherent transport to geometric densification of the activated relational subgraph.

Relation to the Axiomatic Relational–Informational Framework

The present model is not an independent departure from earlier work, but a concrete specialization of the axiomatic relational–informational framework developed in [14].

In that framework, the only primitive object is a relational configuration $G = (V, E, C)$ whose directed edges carry nonnegative constraint weights $C(e)$ interpreted as path-additive informational costs. An informational action $S(G)$, monotone in constraint strength and additive over edges, induces a Gibbs ensemble [20] $P(G) \propto \exp[-\beta S(G)]$, and effective geometry, forces, and spacetime arise as emergent structures of constrained relational accessibility.

In the present work, this general relational structure is specialized to a finite weighted graph with configuration space $\Omega = \{0,1\}^E \times \left(S^1\right)^V$, yielding a mixed discrete–compact Gibbs system in finite volume.

The superconducting-like model introduced here adopts this structure with minimal additional assumptions. First, the relational graph $G = (V, E)$ of Section 2 corresponds to the undirected specialization of the general configuration $G = (V, E, C)$, with baseline transport costs κ_e playing the role of constraint weights $C(e)$. The emergent relational distance $d_{rel}(i, j)$ defined in Equation (1) is the accessibility distance introduced in [14], obtained as minimal cumulative constraint cost along admissible paths. Second, the baseline term S_{base} in Equation (7) is a specific choice of informational action, corresponding to the additive form $S(G) = \alpha \sum_e \Phi(C(e))$ with $\Phi(C) = c$, already shown in [14] to generate well-defined Gibbs ensembles and emergent information geometry.

The additional contributions S_{pair} and S_{phase} do not introduce new ontological primitives; rather, they restrict attention to a particular class of relational configurations in which (i) certain edges may carry an enhanced "low-cost" channel, encoded by binary variables p_{e}, and (ii) vertices carry compact phase degrees of freedom ϕ_{i} that couple only along these low-cost channels. These extra terms are therefore interpreted as a specific physical hypothesis within the axiomatic framework: superconducting behavior corresponds to an emergent organizational phase in which constraint structure and phase alignment co-stabilize, rather than to a modification of the underlying relational principles.

Finally, the statistical weighting $P \propto e^{-\beta S}$ used in Equation (5) is identical in form to the Gibbs ensemble introduced in [14], where β^{-1} is interpreted as an effective noise parameter controlling the exploration of near-optimal relational configurations. In the present context, varying β plays the role of tuning fluctuation strength in the relational network and allows us to distinguish normal, fragile superconducting, and noise-robust superconducting regimes within the same axiomatic architecture.

In the present work, the terminology "low-temperature-like" and "high-temperature-like" refers not to literal thermodynamic temperature, but to the robustness of phase coherence with respect to the effective noise parameter β^{-1} appearing in the informational ensemble. A "low-temperature-like" regime denotes coherence that survives only at large β (weak fluctuations), whereas a "high-temperature-like" regime denotes parameter regions in which macroscopic coherence and phase stiffness persist even at moderate β. This terminology is therefore structural and operational rather than material-specific.

2. Relational Network Model

In this section we introduce the relational model that underlies the results of this work. The construction is deliberately minimal and is designed to extend the axiomatic relational–informational framework in the smallest possible way required to support superconducting behavior. No microscopic particles, quantum fields, or background spacetime structures are assumed. Instead, all physical notions emerge from the organization of constraints and collective degrees of freedom defined on a relational network.

2.1. Network Structure and Relational Distance

The fundamental substrate of the model is a graph $G = (V, E)$ [20,24] where the set of vertices V represents abstract relational sites and the set of edges E represents admissible pathways for transport or information flow between them. This choice follows directly from the axiomatic framework, in which relational adjacency, rather than spatial embedding, is taken as primitive.

Each edge $e \in E$ is assigned a positive baseline cost $\kappa_e > 0$. This cost quantifies the constraint associated with transport across that relation and may be interpreted as

resistance, friction, or informational difficulty. Importantly, κ_e is not an energy in the microscopic sense; it is a structural parameter encoding how easily relational accessibility can be achieved along a given edge.

No notion of geometric distance is assumed a priori. Instead, distance emerges operationally from the constraint structure of the network. The effective distance between two vertices $i,j \in V$ is defined as the minimal cumulative cost along all admissible paths connecting them,

$$d_{rel}(i,j) = \min_{\mathcal{P}_{ij}} \sum_{e \in \mathcal{P}_{ij}} \kappa_e \tag{1}$$

where $\mathcal{P}_{ij}$ denotes a path in the graph from i to j. In this way, geometry arises as a derived, coarse-grained concept rather than as an input. This construction is fully consistent with the relational–informational interpretation of space developed in the axiomatic framework.

It is important to distinguish this emergent, cost-based relational distance d_{rel} from the discrete hop distance used later in numerical measurements of correlation functions. In Section 4, the quantity r denotes the shortest-path length in the underlying adjacency graph of a specific lattice realization (i.e., the minimal number of nearest-neighbor edge traversals between two vertices). This hop distance serves solely as an operational indexing parameter for organizing correlation data in simulations and does not define the fundamental relational geometry of the model.

The relational framework itself remains independent of any predefined metric embedding. The lattice geometry used in simulations is a convenient realization for numerical study; superconducting behavior, if it emerges, arises from the organization of constraints and phase variables on the graph and not from any imposed background spatial structure.

2.2. Emergent Low-Cost Transport Channel

To allow for collective reorganization of transport, each edge $e \in E$ is endowed with an additional binary internal variable

$$p_e \in \{0,1\} \tag{2}$$

This variable represents the activation of a special transport channel on that edge. The interpretation is as follows:

- $p_e = 0$ corresponds to a normal transport channel governed solely by the baseline cost κ_e,
- $p_e = 1$ corresponds to the activation of an additional low-cost channel that facilitates transport across the edge.

The effective cost associated with an edge is then defined as

$$C_{eff}(e) = \kappa_e(1 - \gamma p_e) \tag{3}$$

where $0 < \gamma < 1$ controls the degree to which the special channel reduces the transport cost.

This formulation is chosen for its minimality. The binary variable p_e represents the simplest nontrivial extension of the relational framework that allows transport properties to reorganize dynamically. Continuous-valued channels or multiple internal states are possible generalizations, but they are not required to capture the essential phenomenology of superconductivity explored here.

Crucially, the activation of low-cost channels is not imposed externally. As detailed in Section 3, each active channel carries a cost in the informational action. Low-cost connectivity therefore emerges only when it is collectively favorable at the level of the entire network. This ensures that system-spanning low-resistance pathways arise as an emergent phenomenon rather than as a trivial saturation of edges.

Within the present framework, these low-cost channels play a structural role analogous to paired transport modes in superconductors, but without invoking microscopic pairing mechanisms or particle-based descriptions.

2.3. Phase Degree of Freedom and Coherence

In addition to transport channels, each vertex $i \in V$ is assigned a compact phase variable

$$\phi_i \in [0, 2\pi) \tag{4}$$

These phases represent collective relational degrees of freedom associated with coherence. They are not interpreted as microscopic quantum wavefunctions or order parameters tied to specific particles. Rather, they encode the possibility of phase alignment across extended regions of the network.

The coupling of phase variables is strictly conditional on transport accessibility. Only edges for which the low-cost channel is active ($p_e = 1$) contribute to phase coupling. Edges with $p_e = 0$ do not mediate any phase interaction. This construction ensures that coherence is inseparable from enhanced transport, reflecting the defining property of superconductivity: resistance-free transport and phase coherence arise together.

This choice is conceptually important. It prevents the appearance of spurious long-range order in the absence of efficient transport pathways and guarantees that any macroscopic coherence observed in the system is directly tied to the emergence of low-resistance connectivity.

The phase variables thus provide the minimal additional structure required to distinguish between mere percolation of low-cost pathways and superconducting-like coherent transport behavior, characterized by coherent transport governed by a global phase.

Percolation of low-cost channels and phase coherence play distinct roles in the model. Percolation is a connectivity property of the activated low-cost subgraph and indicates the existence of a system-spanning transport backbone. Phase coherence is an ordering property of the compact vertex phases and indicates whether transport along that backbone is collectively organized rather than locally disordered. The two are therefore not equivalent: a percolating low-cost network may exist without robust long-range coherence, as seen in the fragile regime at low β.

2.4. Conceptual Status of the Model

It is important to emphasize that the relational network model introduced here is not intended as a microscopic description of any specific superconducting material. Instead, it should be understood as a structural extension of the axiomatic relational–informational framework, designed to test whether superconductivity can emerge as a generic phase of constrained relational systems.

All elements of the model—the graph structure, transport costs, low-cost channels, and phase variables—are defined operationally and relationally. No background spacetime, lattice embedding, or particle ontology is assumed. As a result, superconducting behavior, if it arises, does so as an emergent organizational property of the network rather than as a consequence of imposed microscopic dynamics.

This completes the definition of the relational substrate on which the informational action and statistical dynamics, introduced in the next section, are built.

2.5. Notation and Symbol Summary

For clarity, we summarize in Table 1 the main symbols and parameters used throughout the manuscript. All quantities are defined within the relational–informational framework introduced in Sections 2–4.

Table 1. Summary of Symbols and Parameters in the Relational Superconducting Model.

Symbol	Meaning	Type
$G = (V, E)$	Relational graph with vertices V and edges E	Structure
V	Set of relational sites (vertices)	Structure
E	Set of admissible transport relations (edges)	Structure
κ_e	Baseline transport cost of edge e	Parameter
$p_e \in \{0, 1\}$	Binary activation variable for low-cost channel on edge e	Dynamical variable
γ	Cost-reduction factor for activated channels ($0 < \gamma < 1$)	Coupling parameter
$C_{eff}(e)$	Effective transport cost of edge e	Derived quantity
$\phi_i \in [0, 2\pi)$	Phase variable at vertex i	Dynamical variable
J	Phase stiffness coupling constant	Coupling parameter
ϵ_p	Intrinsic activation cost for low-cost channels	Parameter
U	Crowding penalty strength	Parameter
α	Global transport cost weight	Parameter
S	Informational action	Functional
β	Inverse effective noise (fluctuation strength)	Control parameter
ρ_p	Pair density (fraction of edges with $p_e = 1$)	Observable
Largest cluster fraction	Fraction of sites in largest connected low-cost component	Observable
C(r)	Phase correlation function at hop distance r	Observable
r	Graph-theoretic hop distance	Indexing parameter
Y	Helicity modulus (phase stiffness)	Observable
L	Linear system size	Simulation parameter

The symbols in Table 1 should be understood as superconductivity-specific specializations of the more general notation used in the axiomatic relational–informational framework [14]. In particular, the baseline costs κ_e correspond to the constraint weights $C(e)$ of that framework, the emergent relational distance d_{rel} coincides with the accessibility distance defined there, and the informational action S plays the same role of quantifying global constraint tension and inducing a Gibbs ensemble $P \propto e^{-\beta S}$.

3. Informational Action

The relational network introduced in Section 2 acquires physical meaning through its statistical organization. In the axiomatic relational–informational framework, such organization is governed by an action functional that assigns a weight to each admissible configuration of relations and constraints. Geometry, effective forces, and dynamical behavior emerge from the collective minimization of this action under coarse-graining. In the present work, superconducting behavior is likewise treated as an emergent phase arising from the statistical structure of an informational action, rather than from microscopic equations of motion.

We therefore define an effective informational action S that assigns a scalar cost to each configuration of transport channels and phase variables on the network. The action is constructed to be minimal, additive, and fully consistent with the relational principles of the underlying framework. Configurations are sampled according to a Boltzmann weight,

$$P \propto e^{-\beta S} \tag{5}$$

where β controls the strength of fluctuations. Throughout this work, β^{-1} should be interpreted as an effective noise or disorder parameter rather than a literal thermodynamic temperature, although the analogy is useful for interpreting phase transitions.

The total action is written as

$$S = S_{base} + S_{pair} + S_{phase} \tag{6}$$

where each term encodes a distinct structural contribution to the global organization of the network. The separation into these three contributions reflects a conceptual decomposition into transport cost, channel activation, and coherence.

3.1. Baseline Transport Cost

The first contribution to the action accounts for the global cost of transport across the network. It is defined as

$$S_{base} = \alpha \sum_{e \in E} \kappa_e (1 - \gamma p_e) \tag{7}$$

where $\alpha > 0$ sets the overall sensitivity of the system to transport constraints.

This term generalizes the baseline action used in the axiomatic framework, where global tension is measured by the cumulative constraint cost of relational paths. Here, the effective cost of each edge depends on whether the low-cost channel is active. When $p_e = 1$, the contribution of that edge to the global transport cost is reduced, reflecting enhanced accessibility.

Importantly, S_{base} alone does not favor indiscriminate activation of low-cost channels. While activating a channel reduces this contribution to the action, such activation is penalized elsewhere. As a result, reductions in transport cost must be balanced against the energetic cost of creating and maintaining special channels. This balance is essential for preventing trivial solutions in which all edges are activated independently of global structure.

From a relational perspective, S_{base} encodes the tendency of the system to reorganize its constraint structure so as to minimize effective distances between relational sites.

3.2. Pair Creation and Crowding Penalty

The activation and spatial distribution of low-cost transport channels are regulated by the second contribution to the action,

$$S_{pair} = \epsilon_p \sum_{e \in E} p_e + U \sum_{i \in V} \left(\sum_{e \ni i} p_e \right)^2 \tag{8}$$

The first term assigns an intrinsic cost ϵ_p to the activation of each low-cost channel. Positive values of ϵ_p suppress the formation of such channels, while smaller or negative values favor their appearance. This parameter therefore controls the overall density of enhanced transport pathways in the network.

The second term introduces a crowding penalty with strength $U > 0$, which discourages an excessive concentration of low-cost channels around individual vertices. Without this term, the system could reduce its action by clustering many activated edges locally, leading to highly inhomogeneous and unphysical configurations. The quadratic form ensures that low-cost connectivity, when it emerges, does so in a distributed and collective manner across the network.

Together, these terms play a role analogous to regulating the formation and spatial organization of paired transport modes. However, no microscopic pairing mechanism is assumed. The variables p_e encode purely relational possibilities for enhanced accessibility, and their organization is determined statistically by the global action.

3.3. Phase Coherence Term

The third contribution to the action encodes coherence between relational sites and is defined as

$$S_{phase} = -J\sum_{(i,j)\in E} p_{ij}\cos(\phi_i - \phi_j) \quad (9)$$

where $J > 0$ controls the stiffness of phase alignment.

This term favors alignment of phase variables ϕ_i and ϕ_j along edges for which the low-cost channel is active. The cosine form is chosen for its simplicity and periodicity, reflecting the compact nature of the phase variables. Importantly, no phase interaction exists along edges with $p_e = 0$, ensuring that coherence is mediated exclusively by enhanced transport pathways.

This construction embodies a central structural feature associated with superconducting organization: long-range phase coherence cannot exist independently of the emergence of low-cost, low-dissipation transport pathways. In the present framework, coherence and low-cost connectivity are inseparable. Phase alignment is possible only where relational accessibility is sufficiently high.

Although the mathematical form of this term resembles that of an XY-type interaction, its interpretation here is fundamentally relational. The phases do not correspond to microscopic quantum states but to collective degrees of freedom encoding coherence across the network. As a result, macroscopic phase order, when it appears, arises as an emergent organizational feature of the relational system.

3.4. Statistical Interpretation and Phase Structure

The full informational action defines a statistical ensemble of relational configurations. At large β, fluctuations are suppressed and the system organizes into configurations that minimize the action. At smaller β, disorder competes with collective organization, leading to qualitatively different phases.

Within this ensemble, superconducting-like behavior is identified operationally rather than postulated. A superconducting-like phase corresponds to configurations in which low-cost transport channels form a system-spanning connected structure and phase coherence extends across that structure. The distinction between normal conduction, low-temperature-like superconductivity, and high-temperature-like superconductivity arises from how robust this organization is against increasing noise within the ensemble.

This statistical interpretation completes the definition of the model. In the following section, we describe how the resulting ensemble is explored numerically and how superconducting phases are identified using purely relational observables.

4. Simulation Methodology

The relational model defined in Sections 2 and 3 does not admit a closed-form analytical solution in general, due to the coupled, nonlinear dependence between transport channels and phase degrees of freedom. To explore its statistical behavior and emergent phases, we therefore study the model numerically using Monte Carlo simulations [25]. The goal of these simulations is not to reproduce detailed material-specific phenomenology, but to determine whether the relational action supports distinct organizational regimes corresponding to normal conduction, low-temperature superconductivity, and high-temperature superconductivity.

4.1. Choice of Lattice and Boundary Conditions

For numerical concreteness, the relational network $G = (V, E)$ is instantiated as a two-dimensional square lattice with periodic boundary conditions. Each vertex has a fixed

coordination number, and edges connect nearest neighbors. This choice is motivated by two considerations.

First, many superconducting materials, particularly high-temperature cuprates, exhibit strong quasi-two-dimensional character, with transport and coherence dominated by layered structures. Second, a regular lattice provides a controlled setting in which relational distance, connectivity, and correlation functions can be defined unambiguously, while remaining fully consistent with the relational interpretation of the model. Importantly, the formalism itself does not rely on lattice geometry and can be generalized to arbitrary graphs.

Periodic boundary conditions are imposed to reduce boundary effects and to approximate bulk behavior within a finite system. Because the primary simulations are performed on a finite 8×8 lattice, with additional finite-size comparisons on 12×12 and 16×16 lattices discussed later, the results should be interpreted as evidence of extended coherence in finite realizations rather than as a full thermodynamic-limit analysis. A systematic finite-size scaling study would be required to characterize critical behavior in the infinite-system limit and is left for future work.

4.2. Dynamical Variables and Configuration Space

The configuration space of the model consists of two sets of dynamical variables:

1. **Edge variables** $p_e \in \{0, 1\}$, which encode the activation of low-cost transport channels on edges.
2. **Vertex variables** $\phi_i \in [0, 2\pi)$, which encode phase degrees of freedom associated with coherence.

A complete configuration of the system is therefore specified by the pair $\{p_e\}$, $\{\phi_i\}$. Both sets of variables evolve dynamically during the simulation, allowing the network's transport structure and phase organization to co-evolve.

4.3. Monte Carlo Update Scheme

Configurations are sampled from the Boltzmann distribution

$$P \propto e^{-\beta S}$$

where S is the informational action defined in Section 3 and β controls the strength of fluctuations.

We employ a standard Metropolis Monte Carlo algorithm [25,26] consisting of local updates:

- **Edge updates:** an edge e is selected at random and its transport state is proposed to flip, $p_e \to 1 - p_e$.
- **Phase updates:** a vertex i is selected at random and its phase is proposed to change by a small random increment, $\phi_i \to \phi_i + \delta$, where δ is drawn from a symmetric distribution.

Each proposed update is accepted or rejected according to the Metropolis criterion based on the change in the total action ΔS. This update scheme ensures detailed balance and ergodicity within the configuration space.

The separation between edge and phase updates reflects the conceptual structure of the model: transport accessibility and coherence are distinct but coupled degrees of freedom. Allowing both to evolve dynamically is essential for capturing the emergence of superconducting phases.

4.4. Thermalization and Measurement Protocol

Simulations are divided into two stages:

1. **Thermalization:** an initial sequence of Monte Carlo sweeps is discarded to allow the system to relax from its initial condition toward equilibrium.
2. **Measurement:** observables are recorded over subsequent sweeps, with sufficient separation between measurements to reduce autocorrelation effects.

All reported quantities are obtained by averaging over the measurement phase. Where appropriate, simulations are repeated with different random seeds to ensure statistical robustness.

4.5. Observables

Superconducting behavior is identified using observables defined entirely in relational terms, consistent with the axiomatic framework. The primary diagnostics are as follows.

Pair density. The fraction of edges with activated low-cost channels,

$$\rho_p = \frac{1}{|E|}\sum_{e\in E} p_e \tag{10}$$

provides a measure of how extensively enhanced transport pathways populate the network.

Largest connected component. We compute the size of the largest connected cluster formed by edges with $p_e = 1$, normalized by the number of vertices. A cluster that spans a finite fraction of the system indicates percolating low-resistance connectivity.

Phase correlation function. Phase coherence is quantified by the correlation function

$$C(r) = \langle \cos(\phi_i - \phi_j) \rangle \tag{11}$$

where the average is taken over all unordered pairs of vertices (*i*,*j*) separated by graph-theoretic hop distance r. In the present 8×8 periodic square lattice realization, r is defined as the minimal number of nearest-neighbor edge traversals (Manhattan distance on the torus) connecting i and j.

This definition depends only on adjacency relations in the chosen graph and does not assume a continuous background metric. The hop distance serves solely as an operational indexing parameter for organizing correlation data in simulations. Long-range persistence of $C(r)$ as r increases signals macroscopic phase coherence, while rapid decay indicates incoherent transport. For a general graph realization, r would correspond to the shortest-path length in the underlying adjacency graph.

These observables allow a clear operational distinction between different phases of the model without reference to microscopic particles, currents, or electromagnetic response. In this sense, the observables diagnose structural superconducting-like organization within the relational model, rather than full electromagnetic superconductivity.

4.6. Phase Stiffness (Helicity Modulus)

To complement the cluster and correlation-based diagnostics, we also compute an operational phase stiffness (helicity modulus) Υ, which probes the energetic cost of twisting the phase field across the system. In analogy with XY-type models of superconducting films, the helicity modulus along a given direction (say, x) is defined as the second derivative of the free energy with respect to a uniform phase twist imposed along that direction. Operationally, we introduce a small twist θ in the phase differences along x-directed edges, $\phi_i - \phi_j \to \phi_i - \phi_j + \theta$, and estimate

$$\mathrm{Y_x} \approx \frac{1}{\mathrm{L}^2}\frac{\partial^2 \mathrm{F}(\theta)}{\partial \theta^2}\text{evaluated at } \theta = 0 \tag{12}$$

where F(θ) is the effective free energy per site in the presence of the twist and L is the linear system size. In practice, we evaluate this curvature using a finite-difference estimator, comparing the action with and without a small twist applied along x

$$\Upsilon \approx \frac{F(\theta) - 2F(0) + F(-\theta)}{L^2\theta^2} \tag{13}$$

A nonzero positive Υ indicates a phase-stiff state in which global coherence is resistant to distortions, whereas $\Upsilon \simeq 0$ signals the absence of macroscopic stiffness.

In the results below we report Υ as an averaged scalar quantity (dropping the x subscript), since the square lattice with periodic boundary conditions is isotropic at the level of the present model.

4.7. Identification of Phases

A superconducting-like phase is operationally defined as a regime in which:

- low-cost transport channels form a system-spanning connected structure, and
- phase correlations remain long-ranged across that structure.

This definition is structural and operational within the relational model and is not intended as a claim of full microscopic or electromagnetic superconductivity.

A normal conducting phase is characterized by fragmented low-cost connectivity and rapidly decaying phase correlations.

Within the class of superconducting-like phases, a low-temperature-like regime denotes superconducting-like behavior that survives only at large β (weak fluctuations), whereas a high-temperature-like regime denotes parameter regions in which macroscopic coherence and phase stiffness persist over a broad range of β.

4.8. Simulation Parameters and Statistical Analysis

One Monte Carlo sweep is defined as a sequence of |E| attempted edge updates followed by |V| attempted phase updates, where |E| and |V| denote the numbers of edges and vertices, respectively. For all simulations, configurations were initialized with randomly assigned binary channel variables p_e and uniformly distributed phases $\phi_i \in [0, 2\pi)$.

For the L = 8 simulations reported in Tables 2–6, each parameter point (regime, β) was simulated with 500 thermalization sweeps followed by 1000 measurement steps. Between successive measurements, 5 additional sweeps were performed to reduce short-time correlations, for a total of approximately 5500 sweeps per parameter point. Observables were recorded at the end of each measurement block.

Table 2. Representative numerical observables in the strong-coupling regime at neutral pairing field ($\epsilon_p = 0.0$). Shown are the pair density ρ_p, the fraction of lattice sites belonging to the largest connected component of low-cost edges, and the phase correlation function $C(r)$ measured at lattice distances r = 1, 2, 3, as functions of the inverse noise parameter β. Even at β = 1, the system exhibits a nearly system-spanning low-cost network and substantial long-range phase coherence. Increasing β further enhances and saturates both percolation and phase coherence, indicating a robust superconducting phase.

β	ρ_p	Largest Cluster	C(1)	C(2)	C(3)
1.0	0.857	0.999	0.807	0.745	0.710
2.0	0.983	1.000	0.934	0.913	0.901
3.0	0.998	1.000	0.958	0.944	0.937
4.0	1.000	1.000	0.969	0.959	0.953
5.0	1.000	1.000	0.975	0.967	0.962

Table 3. Dependence of the superconducting observables on the pairing field ϵ_p at fixed inverse noise parameter $\beta = 1.0$. Despite a progressive reduction in pair density as ϵ_p increases, the largest low-cost cluster continues to span nearly the entire lattice, and phase correlations remain large and slowly decaying with distance. These results demonstrate that global coherence in the strong-coupling regime is robust against moderate energetic penalties for pair formation.

ϵ_p	Pair Density ρ_p	Largest Cluster Fraction	C(1)	C(2)	C(3)
−0.5	0.911	1.000	0.840	0.790	0.764
0.0	0.861	0.999	0.812	0.762	0.737
+0.5	0.779	0.996	0.766	0.693	0.654

Table 4. Normal regime (N) observables on an 8×8 lattice. Pair density ρ_p, largest low-cost cluster fraction, and phase correlation function $C(r)$ at distances $r = 1, 2, 3$ as functions of β for the weak-coupling parameter set $\gamma = 0.3$, $J = 0.3$, $\epsilon_p = 0.8$, $U = 0.2$ ($\alpha = 1$, $\kappa_e = 1$). The low channel density, subextensive largest cluster, and correlations fluctuating around zero indicate a normal resistive regime with fragmented low-cost connectivity and absent macroscopic phase coherence.

β	ρ_p	Largest Cluster	C(1)	C(2)	C(3)
1.0	0.208	0.096	0.025	−0.001	0.002
2.0	0.108	0.051	0.032	−0.001	0.002
3.0	0.058	0.037	0.021	0.003	0.001
4.0	0.032	0.032	0.017	−0.000	0.002
5.0	0.016	0.030	0.010	−0.002	−0.002

Table 5. Fragile superconducting regime (F) on an 8×8 lattice. Pair density ρ_p, largest low-cost cluster fraction, and phase correlation function $C(r)$ at distances $r = 1, 2, 3$ as functions of β for the intermediate-coupling parameter set $\gamma = 0.7$, $J = 1.0$, $\epsilon_p = 0.2$, $U = 0.1$ ($\alpha = 1$, $\kappa_e = 1$). The low-cost cluster becomes nearly spanning already at $\beta = 1$ and fully spanning by $\beta \geq 3$, while intermediate- and long-range correlations C(2), C(3) are strongly suppressed at $\beta = 1$ and increase rapidly with β. This combination of extended low-cost connectivity and noise-sensitive coherence identifies a fragile superconducting regime.

β	ρ_p	Largest Cluster	C(1)	C(2)	C(3)
1.0	0.490	0.754	0.231	0.076	0.025
2.0	0.566	0.908	0.498	0.322	0.232
3.0	0.673	0.988	0.773	0.692	0.649
4.0	0.722	0.991	0.846	0.783	0.744
5.0	0.766	0.999	0.908	0.876	0.858

To control for sampling variability, all L = 8 results were averaged over 5 independent runs with different random number seeds for each regime and value of β. For a given β, the seed used in the s-th run was taken as

$$seed = base_{seed} + s + [10\beta]$$

with distinct base_seed values for the three regimes to avoid accidental correlations between runs. The quantities reported in Tables 2–5 and in the helicity modulus summary (Table 6) correspond to arithmetic means over these independent realizations.

For the finite-size comparison on a larger L = 12 and L = 16 lattices (Table 7), a lighter Monte Carlo protocol was used for computational efficiency: 150 thermalization sweeps followed by 60 measurement steps, with 2 additional sweeps between measurements. Each (regime, β) point at L = 12 and L = 16 was averaged over 3 independent seeds using the same seeding scheme as above.

Table 6. Helicity modulus Υ and intermediate-distance phase correlation C(2) as functions of β for the three parameter sets N (normal), F (fragile superconducting), and R (noise-robust superconducting) on an 8×8 periodic lattice. All values are averaged over five independent Monte Carlo seeds per parameter point (500 thermalization sweeps followed by 1000 measurement steps with 5 sweeps between measurements). Regime R exhibits a sizable and increasing helicity modulus across the full β range, regime F shows a much smaller and strongly β -dependent stiffness, and regime N has Υ fluctuating around zero. The clear separation $\Upsilon_R > \Upsilon_F \approx 0 > \Upsilon_N$ confirms that the three regimes differ not only in connectivity and correlation structure but also in intrinsic phase rigidity.

Regime	β	C(2)	Υ
F	1.0	0.076	0.006
F	2.0	0.322	0.057
F	3.0	0.692	0.158
F	4.0	0.783	0.199
F	5.0	0.876	0.254
N	1.0	−0.001	−0.001
N	2.0	−0.001	−0.000
N	3.0	0.003	−0.000
N	4.0	−0.000	0.000
N	5.0	−0.002	−0.000
R	1.0	0.745	0.297
R	2.0	0.913	0.460
R	3.0	0.944	0.483
R	4.0	0.959	0.494
R	5.0	0.967	0.497

Phase updates were performed by proposing $\phi_i \to \phi_i + \delta$, where δ was drawn uniformly from the interval $[-0.3, 0.3]$. This fixed step size yielded Metropolis acceptance rates in the range 40–60% across the parameter values explored. Helicity moduli Υ were computed using the finite-difference estimator defined in Equation (13) with twist magnitude $\theta = 0.05$; spot checks at $\theta = 0.03$ and $\theta = 0.07$ produced consistent values within the sampling variability of the Monte Carlo runs.

The aim of the present numerical study is to identify qualitative organizational regimes—normal, fragile superconducting, and noise-robust superconducting—rather than to determine critical exponents or thermodynamic-limit phase boundaries. Within this scope, the averages over 5 seeds at L = 8 and 3 seeds at L = 12 and L = 16 were found sufficient to yield stable mean values of the pair density, largest-cluster fraction, correlation functions, and helicity modulus at the level of precision discussed in Section 5.

Table 7. Finite-size comparison of key observables for L = 8, L = 12, and L = 16 periodic lattices at β = 1 and β = 3 in the normal (N), fragile superconducting (F), and noise-robust superconducting (R) regimes. Shown are the pair density ρ_p, the fraction of lattice sites belonging to the largest connected component of low-cost edges ("Largest cluster fraction"), the intermediate-distance phase correlation C(2), and the helicity modulus ϒ. For L = 8, values are averaged over five independent Monte Carlo seeds per parameter point (500 thermalization sweeps followed by 1000 measurement steps with 5 sweeps between measurements). For L = 12 and L = 16, values are averaged over three independent seeds (150 thermalization sweeps followed by 60 measurement steps with 2 sweeps between measurements). The qualitative hierarchy $\Upsilon_R > \Upsilon_F \approx 0 > \Upsilon_N$ persists under system-size enlargement, indicating that the distinction between normal, fragile superconducting, and noise-robust superconducting regimes reflects structurally different patterns of connectivity and phase rigidity rather than a finite-size artifact of the smallest lattice.

Regime	L	β	ρ_p	Largest Cluster Fraction	C(2)	ϒ
R	8	1.0	0.857	0.999	0.745	0.297
R	12	1.0	0.781	0.997	0.366	0.055
R	16	1.0	0.781	0.997	0.378	0.056
R	8	3.0	0.998	1.000	0.944	0.483
R	12	3.0	0.981	1.000	0.802	0.065
R	16	3.0	0.980	1.000	0.795	0.083
F	8	1.0	0.490	0.754	0.076	0.006
F	12	1.0	0.497	0.734	0.106	0.017
F	16	1.0	0.487	0.629	0.055	−0.003
F	8	3.0	0.673	0.988	0.692	0.158
F	12	3.0	0.599	0.949	0.296	0.019
F	16	3.0	0.605	0.947	0.323	0.044
N	8	1.0	0.208	0.096	−0.001	−0.001
N	12	1.0	0.208	0.051	0.003	−0.002
N	16	1.0	0.211	0.033	−0.003	−0.001
N	8	3.0	0.058	0.037	0.003	−0.000
N	12	3.0	0.057	0.018	0.016	−0.001
N	16	3.0	0.059	0.011	−0.001	0.001

5. Emergent Phases and Numerical Results

In this section we present the numerical results of the relational superconducting model introduced in Sections 2–4. The goal is to identify and characterize three emergent regimes—normal resistive, low-temperature-like (fragile) superconducting-like, and noise-robust superconducting-like, using only relational observables. In particular, we focus on three quantities measured in Monte Carlo simulations on an 8×8 periodic lattice:

- the pair density ρ_p, defined as the fraction of edges with active pair occupation $(p_e = 1)$;
- the largest low-cost cluster fraction, defined as the fraction of lattice sites belonging to the largest connected component of low-cost edges;
- the phase correlation function $C(r) = \langle \cos(\phi_i - \phi_j) \rangle$ where the average is taken over all unordered pairs of vertices separated by graph-theoretic hop distance r (shortest-path length in the periodic square lattice), evaluated for $r = 1, 2, 3$.

Unless otherwise stated, the numerical values reported below correspond to one of three representative parameter sets. The noise-robust superconducting regime (R) is realized by a strong-coupling choice $\gamma = 0.9$, $J = 2.0$, $\epsilon_p = 0.0$, $U = 0.05$ (with $\alpha = 1$ and $\kappa_e = 1$), and is the regime shown in Tables 2 and 3. The normal regime (N) is obtained by suppressing channel formation and coherence $\gamma = 0.3$, $J = 0.3$, $\epsilon_p = 0.8$, $U = 0.2$, while the fragile superconducting regime (F) corresponds to intermediate coupling $\gamma = 0.7$, $J = 1.0$, $\epsilon_p = 0.2$, $U = 0.1$, where low-cost connectivity can percolate but coherence is highly sensitive to noise. All three regimes are generated by the same informational action; only the parameter values differ.

For clarity, the three regimes are defined operationally in terms of the observables introduced above. A configuration is classified as normal (N) if, across the range of β values examined, the largest low-cost cluster fraction remains subextensive (typically below $\approx$0.3) and both the intermediate-distance phase correlation and helicity modulus satisfy $|C(2)| \lesssim 0.05$ and $|\Upsilon| \lesssim 0.01$, indicating fragmented connectivity and the absence of macroscopic stiffness (Table 4). The fragile superconducting regime (F) corresponds to parameter choices for which low-cost connectivity already percolates or nearly percolates (largest cluster fraction $\gtrsim 0.7$ at $\beta \approx 1$) but intermediate- and long-range correlations C(2), C(3) and the helicity modulus Υ are strongly noise-sensitive: they remain small at $\beta = 1$ and increase rapidly only as β is raised (Tables 5 and 6). The noise-robust superconducting regime (R) is characterized by a system-spanning low-cost cluster (largest cluster fraction $\simeq 1$) together with large correlations $C(2) \gtrsim 0.7$ and a clearly positive helicity modulus already at $\beta = 1$, both of which remain sizable and slowly varying as β increases (Tables 2 and 6). In this way, "normal", "fragile superconducting", and "noise-robust superconducting" are distinguished by the joint behavior of connectivity, coherence, and phase stiffness rather than by parameter values alone.

5.1. Noise-Robust Superconducting Regime (R): Representative Numerical Values

We begin by summarizing representative numerical values for the strong-coupling regime at neutral pairing field $\epsilon_p = 0.0$. Table 2 lists the pair density, largest cluster fraction, and phase correlations as functions of the inverse noise parameter β.

Several features are immediately apparent. Even at the lowest value $\beta = 1$, corresponding to strong fluctuations, the system already exhibits a nearly system-spanning low-cost network and substantial phase coherence extending to the largest measured distance. As β increases, both the pair density and the phase correlations rapidly saturate, indicating a robust superconducting phase.

5.2. Dependence on the Pairing Field ϵ_p

To probe the sensitivity of the superconducting phase to the pairing field, we next fix $\beta = 1$ and vary ϵ_p. The results are summarized in Table 3.

Even when pair formation is penalized ($\epsilon_p = 0.5$), the system remains in a superconducting state: the largest cluster continues to span almost the entire lattice, and phase correlations remain large and slowly decaying with distance. The pairing field primarily affects the quantitative values of ρ_p and $C(r)$, but does not destroy global coherence in this strong-coupling regime.

5.3. Normal and Fragile Superconducting Regimes

To demonstrate that the same relational action supports not only a noise-robust superconducting regime but also normal and fragile-superconducting behavior, we now compare the strong-coupling results of Tables 2 and 3 with two additional parameter sets.

Table 4 reports observables for the weak-coupling set **N** ($\gamma = 0.3$, $J = 0.3$, $\epsilon_p = 0.8$, $U = 0.2$). Here the pair density ρ_p decreases from $\approx$0.21 at $\beta = 1$ to $\approx$0.02 at $\beta = 5$, the

largest low-cost cluster fraction remains in the range 0.03–0.10, and the correlations C(1), C(2), and C(3) fluctuate around zero. This combination of low channel density, non-spanning connectivity, and absence of sustained phase correlations is characteristic of a normal resistive regime, in which low-cost pathways remain fragmented and macroscopic coherence does not develop.

In contrast, Table 5 shows the intermediate-coupling set **F** ($\gamma = 0.7$, $J = 1.0$, $\epsilon_p = 0.2$, $U = 0.1$). At $\beta = 1$ the pair density is already moderate ($\rho_p \approx 0.49$) and the largest low-cost cluster covers ≈0.76 of the lattice, yet C(2) and C(3) remain small (≈0.08 and ≈0.03, respectively), indicating limited coherence beyond nearest neighbors. As β increases from 1 to 5, both the cluster fraction and correlations increase monotonically: the largest low-cost cluster becomes essentially spanning by $\beta \geq 3$, and C(2), C(3) rise to ≈0.88 and ≈0.86 at $\beta = 5$. This regime therefore combines extended low-cost connectivity with coherence that is highly sensitive to fluctuations, providing a clear example of a fragile superconducting phase within the same relational model.

The fragile regime therefore makes explicit that percolation is necessary but not sufficient for superconducting-like behavior in the present framework: extended low-cost connectivity can be present even when phase coherence remains weak and strongly noise-sensitive.

5.4. Phase Stiffness Across Regimes on an 8 × 8 Lattice

The pair density, cluster fraction, and correlation functions discussed above capture connectivity and coherence, but do not directly probe the energetic rigidity of the phase field. To quantify phase stiffness, we compute the helicity modulus Υ as described in Section 4.6 for all three parameter sets N, F, and R on the 8 × 8 lattice. Table 6 reports Υ as a function of β, together with the intermediate-distance correlation C(2) for reference. All values are averaged over five independent Monte Carlo seeds per parameter point (see Section 4.8).

In the noise-robust regime R, the helicity modulus is clearly positive and increases from $\Upsilon \approx 0.297$ at β = 1 to $\Upsilon \approx 0.497$ at β = 5, mirroring the already large and saturating values of C(2) (from C(2) ≈ 0.745 at β = 1 to C(2) ≈ 0.967 at β = 5). This behavior indicates a genuinely phase-stiff state in which macroscopic coherence is energetically protected against distortions.

In the fragile regime F, Υ remains very small at low β ($\Upsilon \approx 0.006$ at β = 1) despite partial connectivity and only reaches moderate values ($\Upsilon \approx 0.254$ at β = 5). Although C(2) becomes large at high β (≈0.876 at β = 5), the corresponding stiffness remains substantially lower than in regime R. Phase coherence in F is therefore much less rigid and significantly more sensitive to fluctuations, consistent with its interpretation as a fragile or low-temperature-like superconducting phase.

In the normal regime N, Υ fluctuates around zero across the entire β range (e.g., $\Upsilon \approx -0.001$ at β = 1 and effectively zero at higher β), consistent with the near-vanishing intermediate-distance correlations reported in Table 4. Together, these results show that the three relational regimes differ not only in connectivity and correlation structure, but also in their intrinsic phase rigidity.

5.5. Percolation of Low-Cost Transport Channels

A necessary condition for superconductivity in the relational framework is the existence of a system-spanning network of low-cost transport channels. Figure 1 shows the fraction of sites belonging to the largest low-cost cluster as a function of β for $\epsilon_p = -0.5$, 0.0, 0.5.

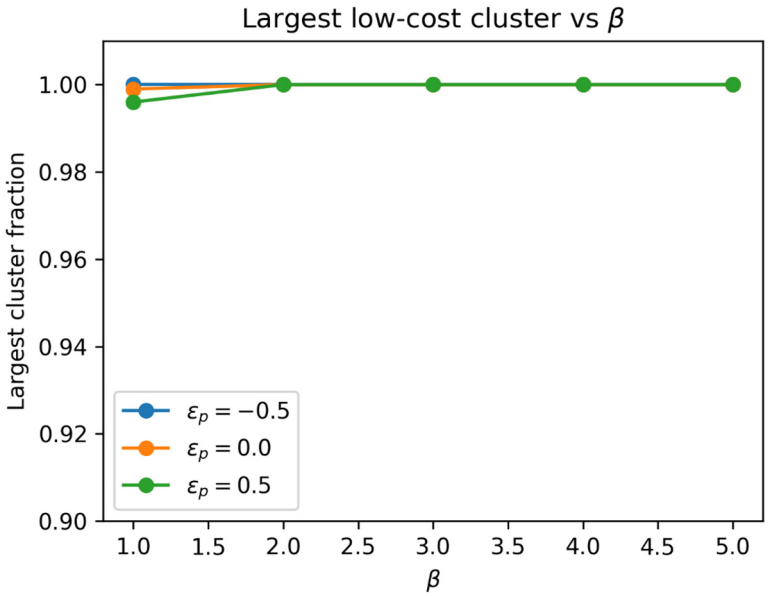


Figure 1. Fraction of lattice sites belonging to the largest connected component of low-cost edges as a function of the inverse noise parameter β for three values of the pairing field ϵ_p. For all parameter values shown, the largest cluster occupies essentially the entire lattice, indicating the formation of a robust, system-spanning network of low-cost transport channels. This percolation behavior is a necessary condition for superconductivity in the relational framework.

As seen in Figure 1, the cluster fraction is essentially equal to unity for all values of β and ϵ_p considered. This indicates that once the strong-coupling regime is entered, the low-cost edges percolate across the entire lattice and form a robust transport backbone [19,27]. In contrast, in the normal regime N (Table 4), the largest low-cost cluster fraction remains well below unity and no system-spanning network forms.

Correlations were evaluated up to $r = 3$, which already spans a significant fraction of the 8×8 lattice extent.

5.6. Spatial Structure of Phase Coherence

Percolation alone is not sufficient for superconductivity: the phases associated with the transport channels must also be coherent over long distances. To probe this, we examine the phase correlation function C(r).

Figure 2 shows C(r) at distances $r = 1, 2, 3$ for $\epsilon_p = 0$ and three representative values of β.

At $\beta = 1$, the correlation decreases modestly with distance but remains substantial even at $r = 3$. As β increases, the decay becomes extremely weak: for $\beta = 3$, the values of C(1), C(2), and C(3) differ by less than a few percent. This behavior is characteristic of long-range phase coherence and clearly distinguishes the superconducting regime from the normal phase, where correlations decay rapidly with distance.

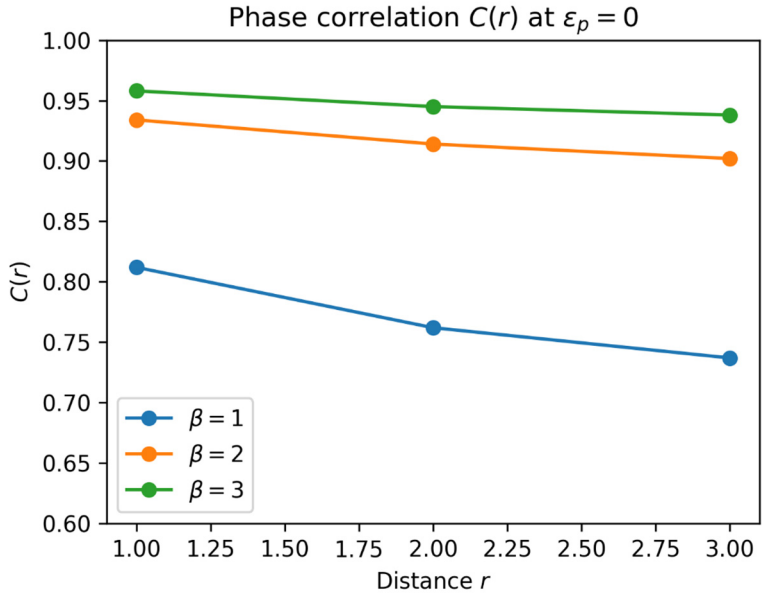


Figure 2. Phase correlation function C(r) = ⟨cos(ϕi − ϕj)⟩ as a function of lattice distance r for ϵ_p = 0 and three representative values of the inverse noise parameter β. Even at the highest noise level considered (β = 1), phase correlations decay only moderately with distance. At larger β, the decay becomes extremely weak, with correlations remaining close to unity over the entire measured range, demonstrating long-range phase coherence.

5.7. Robustness of Coherence Against Noise

To quantify the robustness of superconductivity against fluctuations, we focus on the intermediate-distance correlation C(2), which provides a sensitive probe of coherence beyond nearest neighbors. Figure 3 shows C(2) as a function of β for the three values of ϵ_p.

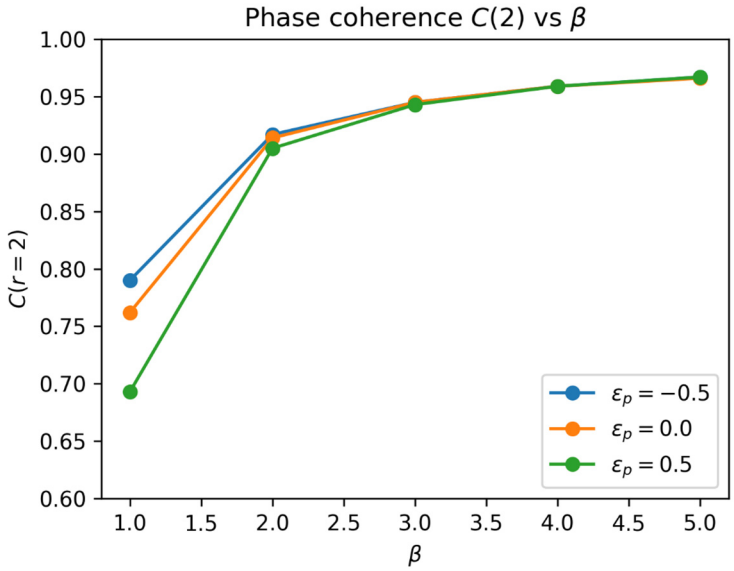


Figure 3. Intermediate-distance phase coherence C(r = 2) as a function of the inverse noise parameter β for three values of the pairing field ϵ_p. For all ϵ_p, coherence remains substantial even at β = 1 and increases smoothly with β, saturating near unity. The weak dependence on ϵ_p highlights the structural robustness of the superconducting phase against both fluctuations and variations in pairing energetics.

For all ϵ_p, C(2) remains large even at β = 1, with values between approximately 0.69 and 0.79. As β increases, C(2) rises smoothly and saturates near 0.96. The weak dependence on ϵ_p and the persistence of large correlations at low β indicate that coherence

is structurally stabilized in this regime. In the dimensionless units of the model, this behavior justifies referring to the strong-coupling case as a structurally noise-robust, high-temperature-like superconducting regime in the operational sense defined above.

5.8. Finite-Size Robustness: Comparison Between 8 × 8, 12 × 12 and 16 × 16 Lattices

To assess whether the observed phase structure is an artifact of the smallest system size, we performed additional simulations on larger 12 × 12 and 16 × 16 periodic lattices for representative values $\beta = 1$ and $\beta = 3$ in all three regimes N, F, and R, using the same parameter sets as in Tables 2–5. Results are averaged over three independent Monte Carlo seeds per parameter point for L = 12 and L = 16 (see Section 4.8). Table 7 summarizes the comparison between L = 8, L = 12, and L = 16 for the pair density ρ_p, the largest low-cost cluster fraction, the intermediate-distance correlation C(2), and the helicity modulus Υ.

In the noise-robust superconducting regime R, the low-cost cluster remains essentially spanning at all three sizes. At $\beta = 1$, the largest cluster fraction decreases slightly from 0.999 (L = 8) to 0.997 (L = 12 and L = 16), while C(2) decreases from 0.745 (L = 8) to ≈0.37 (L = 12–16). The helicity modulus shows a strong reduction between L = 8 and L = 12 (from 0.297 to 0.055) but then stabilizes between L = 12 and L = 16 (0.055 versus 0.056). A similar pattern is observed at $\beta = 3$: the largest cluster fraction remains equal to unity for all sizes, C(2) decreases from 0.944 (L = 8) to ≈0.80 (L = 12–16), and Υ drops from 0.483 (L = 8) to 0.065 (L = 12) and then remains clearly positive at L = 16 (0.083). These trends indicate that the strong suppression of Υ between L = 8 and L = 12 reflects finite-size renormalization from very small lattices, while the persistence of a positive helicity modulus at L = 16 supports the interpretation of regime R as a phase-stiff relational regime in finite systems.

In the fragile superconducting regime F, extended low-cost connectivity persists under system-size enlargement, but phase stiffness remains much more weakly developed and sensitive to lattice size. At $\beta = 1$, the largest cluster fraction decreases from 0.754 (L = 8) to 0.734 (L = 12) and 0.629 (L = 16), with C(2) remaining small (0.076, 0.106, and 0.055, respectively), while Υ fluctuates around zero (0.006, 0.017, and -0.003). At $\beta = 3$, connectivity is nearly spanning at all sizes (largest cluster fractions of 0.988, 0.949, and 0.947), and C(2) increases from ≈0.30 (L = 12) to ≈0.32 (L = 16), but the helicity modulus remains much smaller than in regime R (0.158 at L = 8, 0.019 at L = 12, and 0.044 at L = 16). This behavior is consistent with a fragile or low-temperature-like superconducting regime in which coherence can develop but is far less rigid and more strongly size- and noise-sensitive than in the noise-robust regime.

In the normal regime N, both connectivity and stiffness remain suppressed across all sizes. At $\beta = 1$, the largest cluster fraction decreases from 0.096 (L = 8) to 0.051 (L = 12) and 0.033 (L = 16), while C(2) fluctuates near zero and Υ remains effectively zero. At $\beta = 3$, the largest cluster fraction remains subextensive (0.037, 0.018, and 0.011 for L = 8, 12, and 16, respectively), and both C(2) and Υ stay at noise level. The normal regime therefore exhibits neither system-spanning connectivity nor macroscopic phase stiffness.

Overall, the qualitative hierarchy

$$\Upsilon_R > \Upsilon_F \approx 0 > \Upsilon_N$$

persists under system-size enlargement from L = 8 to L = 16. The strong-coupling regime retains a clearly positive helicity modulus and extended correlations at all sizes studied, the fragile regime exhibits connectivity without robust stiffness, and the normal regime remains incoherent. With only three lattice sizes, we do not attempt a thermodynamic extrapolation of $\Upsilon(L)$; instead, the present comparison shows that the three relational regimes correspond to distinct patterns of connectivity and phase rigidity that are already clearly manifested in finite systems of moderate size. The apparent partial stabilization of Υ between L = 12

and L = 16 should therefore be interpreted only as evidence that the qualitative regime hierarchy persists across the finite sizes studied, not as proof of asymptotic convergence.

5.9. Summary of Phase Behavior

The numerical results presented in this section reveal a clear and consistent picture of emergent phases in the relational model. In the normal regime N (Table 4), low-cost edges fail to percolate and phase correlations remain essentially at noise level, leading to incoherent transport. In the fragile superconducting regime F (Table 5), low-cost edges already form an extended, nearly spanning backbone at $\beta \approx 1$ but macroscopic coherence is strongly noise-sensitive, with C(2) and C(3) suppressed at low β and recovering only as fluctuations are reduced. In contrast, the strong-coupling regime R exhibits a system-spanning network of low-cost channels (Figure 1), large and slowly decaying phase correlations (Figure 2), and remarkable robustness of coherence against noise (Figure 3). Importantly, all of these behaviors arise from the same relational action, without introducing distinct microscopic mechanisms for different superconducting regimes. The distinction between normal, low-temperature superconducting, and high-temperature-like superconducting behavior emerges dynamically from the organization of constraints and phase stiffness within the relational network.

All numerical results presented here are obtained on a finite 8×8 periodic lattice. While the persistence of large cluster fractions and slowly decaying correlations across the full system indicates extended coherence within this finite realization, we do not claim to have established true long-range order in the strict thermodynamic sense. The present results should therefore be understood as demonstrating structural regimes of connectivity and phase organization within a minimal relational system, rather than as a complete finite-size scaling analysis.

5.10. Schematic Phase Diagram of Relational Superconducting-like Regimes

The numerical results obtained for the three representative parameter sets N, F, and R suggest a qualitative phase structure in the space of effective noise (β^{-1}) and coupling strength (as controlled by γ and J). Although a full parameter sweep and finite-size scaling analysis would be required to determine sharp phase boundaries, the present results allow construction of a schematic phase diagram summarizing the organizational regimes supported by the relational action.

Figure 4 illustrates this qualitative structure. At weak coupling (low γ and J), the system remains in a normal resistive regime for all values of β, characterized by fragmented low-cost connectivity, near-zero phase correlations, and vanishing helicity modulus. At intermediate coupling, a fragile superconducting regime emerges: low-cost transport channels can percolate across the system, but long-range coherence and phase stiffness are strongly suppressed at low β and recover only as fluctuations decrease. At strong coupling, a noise-robust superconducting regime appears, in which system-spanning connectivity, large phase correlations, and a clearly positive helicity modulus persist even at substantial noise levels.

The comparison between 8×8, 12×12 and 16×16 lattices shows that this hierarchy—normal, fragile superconducting, and noise-robust superconducting—is structurally stable under system-size enlargement, supporting the interpretation of these regimes as intrinsic features of the relational architecture rather than artifacts of the smallest lattice realization.

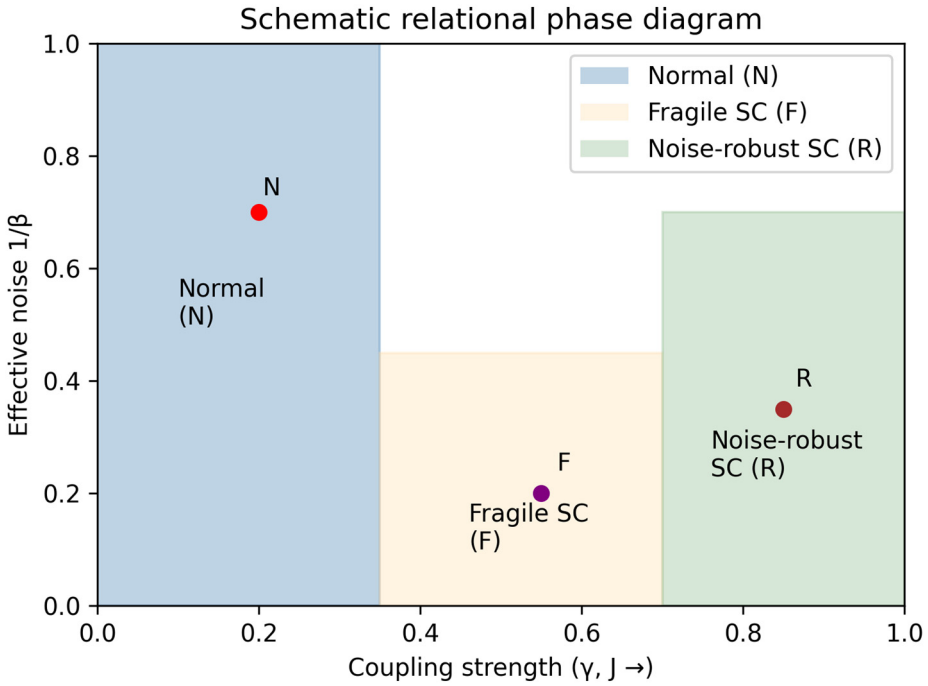


Figure 4. Schematic phase diagram of the relational superconducting model in the plane of effective noise (β^{-1}) and coupling strength (controlled by γ and J). Three organizational regimes are supported by the same informational action: a normal resistive phase at weak coupling, a fragile superconducting phase at intermediate coupling in which coherence is strongly noise-sensitive, and a noise-robust superconducting phase at strong coupling where system-spanning connectivity, large phase correlations, and nonzero helicity modulus persist even at substantial noise. The diagram is qualitative and summarizes the numerical evidence presented in Tables 2–7.

5.11. Relational Ball Growth and Effective Geometric Dimension

To make explicit the geometric reorganization underlying the three emergent regimes, we analyze the growth of relational balls within the subgraph formed by low-cost edges ($p_e = 1$). For each Monte Carlo configuration at β = 1 on the L = 8 lattice, we select vertices belonging to the largest low-cost connected component and define B(r) as the number of vertices reachable within graph-theoretic hop distance r along low-cost edges only. The quantity ⟨B(r)⟩ is then averaged over vertices and independent Monte Carlo seeds.

If the low-cost subgraph behaves as an effectively d-dimensional extended geometry, one expects [28]

$$B(r) \sim r^{d_{eff}}$$

allowing extraction of an effective geometric dimension d_eff from a log–log fit of ⟨B(r)⟩ versus r.

The results reveal a clear hierarchy across regimes. In the normal regime (N) at β = 1, ball growth is slow and rapidly saturating, yielding $d_{eff} \approx 0.63$. This sublinear scaling reflects fragmented and filamentary connectivity, consistent with the absence of macroscopic coherence and vanishing helicity modulus.

In the fragile superconducting regime (F), ball growth is more extended but still significantly subquadratic, with $d_{eff} \approx 1.09$. The low-cost network forms an extended backbone, but its geometry remains effectively quasi-one-dimensional at this noise level, mirroring the strong noise sensitivity of phase stiffness observed in Table 6.

In contrast, the noise-robust superconducting regime (R) exhibits substantially faster growth, with $d_{eff} \approx 1.48$. Although still below the embedding dimension d = 2 due to finite-size effects and incomplete filling at β = 1, this scaling indicates a much denser and

more homogeneous low-cost geometry. The extended relational accessibility in regime R is consistent with its large phase correlations and clearly positive helicity modulus.

These results demonstrate that the transition from normal to superconducting behavior is accompanied not only by percolation and phase alignment, but also by a qualitative geometric reorganization of the relational network. Superconductivity in this framework therefore corresponds to an emergent geometric phase in which low-cost accessibility becomes extended and increasingly space-filling, supporting robust macroscopic coherence.

6. Discussion

The numerical results presented in Section 5 demonstrate that superconducting behavior can emerge generically within a relational–informational framework, without invoking microscopic particles, lattice vibrations, or material-specific interactions. In this section, we interpret these results by explicitly linking the observed numerical trends to the defining physical features of superconductivity, as evidenced in Tables 2 and 3 and Figures 1–3. We then clarify how both conventional and high-temperature superconductivity arise naturally as different regimes of the same emergent relational phenomenon.

6.1. Superconductivity as an Emergent Relational Phase

Within the present framework, superconductivity is identified operationally by the simultaneous emergence of two macroscopic properties: a system-spanning network of low-cost transport channels and long-range phase coherence across that network. These properties are not imposed but arise dynamically from the statistical organization of constraints encoded in the informational action. The nonzero helicity modulus Υ in the noise-robust regime R, contrasted with $\Upsilon \simeq 0$ in the normal regime N, supports the identification of a phase-stiff relational regime in the operational sense just defined: a configuration is "superconducting" when a system-spanning low-cost backbone coexists with extended phase coherence across that backbone.

This identification is directly supported by the numerical data. As shown in Table 2, the largest low-cost cluster fraction approaches unity across the entire range of inverse noise values $\beta = 1$ to 5, while the phase correlations C(1), C(2), and C(3) remain large and only weakly dependent on distance. Figure 1 makes this percolation behavior explicit: for all values of the pairing field ϵ_p, the low-cost network spans essentially the entire lattice, indicating global accessibility for transport.

In relational terms, superconductivity corresponds to a regime in which effective distances across the network remain bounded even over large separations, while phase coherence suppresses dissipative scrambling. It is important to emphasize that the term "superconductivity" is used here in a structural and operational sense: namely, the coexistence of system-spanning low-cost transport channels and extended phase coherence within a relational network. The present model does not include electromagnetic gauge fields, magnetic flux degrees of freedom, or explicit current–voltage response functions, and therefore does not reproduce hallmark electromagnetic phenomena such as the Meissner effect or flux quantization. Rather, it isolates the minimal relational conditions under which resistance-free, phase-coherent transport becomes structurally possible. In this sense, the model should be understood as identifying a geometric and organizational substrate for superconductivity, not as a complete microscopic theory of any specific material.

The possibility of low-dissipation, phase-coherent transport thus appears not as a microscopic assumption but as a macroscopic consequence of relational organization.

6.2. Low-Temperature Superconductivity as a Fragile Relational Regime

The normal and fragile regimes summarized in Tables 4 and 5 place the strong-coupling results of Section 5.1 in a broader relational context. In the normal regime N, low-cost edges form only small, non-spanning clusters and the correlations C(1), C(2), and C(3) remain close to zero across all β, indicating that coherence never extends beyond local fluctuations. From a relational standpoint, the network fails to organize a low-cost backbone or a coherent phase field, and transport remains effectively resistive.

The fragile superconducting regime F exhibits a qualitatively different pattern. As shown in Table 5, the low-cost cluster already covers a large fraction of the system at $\beta = 1$ (cluster fraction ≈ 0.76) and becomes essentially spanning by $\beta \geq 3$, while ρ_p increases smoothly from $\approx$0.49 to $\approx$0.77. However, the intermediate- and long-range phase correlations C(2) and C(3) are strongly suppressed at $\beta = 1$ ($\approx$0.08 and $\approx$0.03, respectively) and only approach the robust values seen in the strong-coupling regime R for larger β. Small increases in effective noise therefore fragment phase alignment even when low-cost connectivity remains extended.

This behavior captures the defining feature of low-temperature-like superconductivity within the relational framework: coherence exists but is fragile. The network can support a coherent configuration only when fluctuations are strongly suppressed. Modest increases in noise destroy long-range phase alignment or disrupt its percolation across the low-cost backbone, leading to a rapid loss of superconducting behavior. This interpretation mirrors the phenomenology of conventional low-T_c superconductors, which require strong cooling to suppress thermal fluctuations, but here fragility arises purely from the statistical organization of relational constraints and their sensitivity to noise. The small and strongly β-dependent values of Υ in regime F, together with their sensitivity to system size, make this fragility quantitatively explicit.

6.3. High-Temperature-like Superconductivity as a Structurally Stabilized Phase (Regime R)

The strong-coupling parameter set R introduced in Section 5 exhibits behavior that is qualitatively distinct from both the normal regime N (Table 4) and the fragile superconducting regime F (Table 5). As shown in Tables 2 and 3, the largest low-cost cluster fraction remains essentially unity across the entire range β = 1–5, and the phase correlations C(1), C(2), and C(3) remain large even at the highest noise level considered ($\beta = 1$). In particular, C(2) $\approx$ 0.76 already at $\beta = 1$ and increases smoothly toward $\approx$0.97 as β increases, indicating that intermediate-range coherence is not strongly suppressed by fluctuations.

This robustness contrasts sharply with regime F, where the largest cluster becomes nearly spanning already at $\beta \approx 1$ but C(2) and C(3) are strongly reduced at that noise level (Table 5), and with regime N, where both the cluster fraction and all correlations remain small (Table 4). In regime R, connectivity and coherence reinforce one another across the full β range.

Equally important is the spatial structure of coherence. Figure 2 shows that, for $\epsilon_p = 0$ in regime R, the phase correlation function C(r) decays only weakly with distance even at $\beta = 1$. For larger β, the differences between C(1), C(2), and C(3) become minimal, indicating extended phase alignment across the entire 8×8 lattice rather than merely short-range order.

In the dimensionless units of the model, this behavior corresponds to a structurally stabilized, high-temperature-like superconducting regime: long-range coherence persists even under substantial fluctuations within the finite systems studied. Coherence is therefore not a marginal or finely tuned effect in this parameter region but a structurally stabilized property of the relational architecture. The network self-organizes into a dense and redundant configuration in which a system-spanning low-cost backbone supports robust

phase alignment. This is reflected in the helicity modulus of regime R, which, although significantly renormalized between 8×8 and 12×12 lattices, remains clearly positive and stabilizes upon further enlargement to 16×16. This behavior indicates that the observed phase stiffness is not confined to the smallest system size but persists across moderate lattice scales.

6.4. Continuity Between Normal, Fragile, and Noise-Robust Superconductivity

A central implication of these results is that no qualitative change in the underlying model is required to move between the normal, fragile superconducting, and noise-robust superconducting regimes. All three arise from the same informational action and differ only in parameter values controlling cost reduction, channel density, and phase stiffness. The normal regime N corresponds to weak coupling, where channel activation is strongly penalized and phase stiffness is small. The fragile regime F corresponds to intermediate coupling, where low-cost connectivity can percolate but coherence is highly noise-sensitive. The noise-robust regime R corresponds to strong coupling, where both connectivity and coherence are structurally stabilized.

Within each of these parameter regions, changes in the effective noise level β do not induce abrupt qualitative changes in the observables; instead, connectivity and coherence vary smoothly, as illustrated by the gradual evolution of ρ_p, the largest-cluster fraction, and C(2) in Tables 2–5 and Figures 1–3. The distinction between low-temperature-like and high-temperature-like superconductivity therefore appears as a difference in structural stability rather than in microscopic mechanism: fragile superconductors occupy parameter regions where coherence is easily disrupted by fluctuations, whereas high-T_c-like behavior corresponds to regions in which the relational architecture strongly favors dense connectivity and robust phase alignment.

6.5. Relation to Existing Theoretical Approaches

The present framework shares qualitative similarities with several established approaches while remaining conceptually distinct. The emphasis on phase coherence echoes the central role of the macroscopic superconducting phase in BCS theory and in XY-type models. The emergence of superconductivity through percolating structures resembles network and granular models, in which global coherence arises from connectivity.

However, the relational–informational approach differs fundamentally in that it does not presuppose electrons, quasiparticles, or even a background spatial geometry. Transport, coherence, and geometry all emerge from the same underlying organization of constraints. In this sense, the present work does not compete with microscopic theories but complements them by addressing superconductivity at a structural and axiomatic level.

More broadly, the present construction may be viewed in the spirit of emergence frameworks in many-body physics, where effective large-scale organization is not imposed directly but arises from constrained microscopic or relational degrees of freedom. In this limited methodological sense, it is conceptually adjacent to approaches such as string-net condensation, where collective organization gives rise to effective long-wavelength structures. The analogy should not be overstated: the present model does not generate topological order, emergent gauge bosons, or a quantum effective field theory. Its relevance here is instead to illustrate how a simple constrained substrate can support qualitatively new transport and coherence regimes at larger scales.

6.6. Limitations and Scope

The model studied here is intentionally minimal. It does not include electromagnetic fields, fermionic statistics, or dynamical gauge degrees of freedom, and therefore cannot

reproduce material-specific observables such as Meissner expulsion, isotope effects, or spectroscopic signatures.

The significance of the present results lies instead in demonstrating that coherent, low-dissipation transport can emerge generically within a relational framework consistent with an axiomatic approach to physics. The figures and tables in Section 5 show that neither microscopic pairing mechanisms nor predefined spacetime structures are required at the fundamental level for superconducting behavior to arise.

The numerical exploration was performed on finite lattices of size 8×8, 12×12, and 16×16. While the helicity modulus exhibits strong renormalization between the smallest and intermediate sizes, its stabilization between 12×12 and 16×16 in the noise-robust regime suggests a partial finite-system stabilization over the limited size range examined, rather than establishing asymptotic convergence. Nevertheless, a systematic finite-size scaling analysis would be required to determine the precise asymptotic behavior in the thermodynamic limit [29], and this remains an important direction for future investigation. The present study establishes the existence of distinct organizational regimes within a minimal finite relational system; no claim is made here about universality classes, critical exponents, or sharp thermodynamic phase transitions.

In particular, the model does not currently incorporate coupling to an external gauge field. As a result, it cannot reproduce hallmark electromagnetic signatures of superconductivity such as the Meissner effect, London penetration depth, or flux quantization. The present framework captures structural phase coherence and low-resistance transport within a relational network, but a full connection to electromagnetic superconductivity would require extending the informational action to include emergent gauge degrees of freedom and phase stiffness under external twists.

The inclusion of an explicit helicity modulus in the present analysis should be viewed as a first step toward connecting relational phase coherence to standard measures of superfluid and superconducting rigidity; a full treatment of electromagnetic response would require coupling the relational phases to emergent gauge degrees of freedom.

6.7. Conceptual Implications

Taken together, the numerical results and their interpretation suggest that superconductivity should be understood as a structural phase of relational systems, on the same conceptual footing as emergent geometry and effective forces. High-temperature-like superconducting behavior, in particular, appears as a regime in which coherence is not fragile but structurally stabilized by the organization of constraints.

From this perspective, the challenge posed by high-Tc materials is reframed. Rather than asking which exotic microscopic interaction is responsible, one may ask how physical systems realize relational structures that favor dense connectivity and robust phase coherence. The present work provides a proof of principle that such structures are sufficient to generate superconducting behavior, independent of microscopic details.

7. Conclusions

In this work, we have shown that superconducting behavior can emerge generically within a relational–informational framework, without assuming microscopic particles, predefined spacetime geometry, or material-specific pairing mechanisms. By extending an axiomatic relational model to include dynamically activated low-cost transport channels and conditional phase coherence, we demonstrated that low-dissipation, phase-coherent transport arises naturally as a collective organizational phase of constrained relational systems.

Using Monte Carlo simulations on a minimal two-dimensional lattice realization, we identified a robust superconducting regime characterized by jointly emergent system-spanning low-cost connectivity and long-range phase coherence. These features were quantified using purely relational observables, including the fraction of sites belonging to the largest connected low-cost cluster, the phase correlation function C(r), and an operational phase stiffness (helicity modulus). In the strong-coupling regime explored here, both connectivity and coherence persist across a wide range of fluctuation strengths, corresponding—in the dimensionless units of the model—to a high-temperature-like superconducting regime in the structural sense defined in the main text. Finite-size comparison between 8×8, 12×12 and 16×16 lattices confirms that the hierarchy of normal, fragile superconducting, and noise-robust superconducting regimes is structurally stable under system-size enlargement. We do not claim to have established a sharp thermodynamic phase transition or universality class; the present analysis concerns structurally distinct regimes of connectivity and phase organization in finite relational systems.

A central result of this study is that no qualitative change in the underlying relational principles is required to move between normal conduction and superconductivity, or between low-temperature-like and high-temperature-like superconducting behavior. All regimes arise from the same informational action. Differences in transport properties reflect quantitative shifts in the balance between transport cost reduction, channel activation penalties, and phase stiffness, rather than the introduction of distinct microscopic mechanisms.

Crucially, superconducting behavior in the present framework is accompanied by a measurable geometric reorganization of the relational network. Analysis of relational ball growth reveals a monotonic increase in effective geometric dimension from the normal to the fragile and noise-robust superconducting regimes. This demonstrates that superconductivity corresponds not only to percolation and phase alignment, but also to an emergent extension and densification of relational accessibility. In this sense, superconductivity appears as a geometric phase of constrained relational organization.

From a conceptual standpoint, these results reinforce the view that superconductivity, like geometry and effective forces, can be understood as an emergent organizational property of constrained relational systems. Within this framework, high-temperature-like superconductivity appears not as an exceptional mechanism, but as a regime in which coherence is structurally stabilized by the global organization of constraints. This does not replace microscopic theories of specific materials; rather, it suggests that the robustness of high-Tc behavior may reflect deeper structural features of relational architecture that can, in principle, be realized by different microscopic substrates.

The model studied here is intentionally minimal and abstract. It does not incorporate electromagnetic gauge fields, fermionic statistics, or material-specific degrees of freedom, and it is not intended to reproduce detailed experimental observables such as the Meissner effect or spectroscopic gaps. Its purpose is foundational: to demonstrate that superconductivity can arise generically within a relational–informational framework consistent with an axiomatic approach to physics.

Several natural directions for future work follow. A systematic exploration of parameter space would allow explicit mapping of phase boundaries. Extensions to disordered, weighted, or non-Euclidean graphs would test the generality of the relational mechanism. Coupling the phase variables to emergent gauge fields and studying the response to imposed phase twists may allow investigation of London-type equations within a relational setting and provide a bridge toward experimentally realizable systems.

In summary, this work establishes that superconductivity—understood here as resistance-free, phase-coherent transport—can be modeled as a robust emergent phase

of relational organization. By shifting the focus from microscopic mechanisms to structural sufficiency and geometric reorganization, it opens a complementary pathway for understanding superconductivity within a relational foundation for physics.

Author Contributions: Conceptualization, C.G.B., M.A. and D.M.; methodology, C.G.B., B.B. and V.N.; software, B.B. and C.G.B.; validation, D.M., V.N. and F.N.; formal analysis, C.G.B., M.A. and I.G.S.; investigation, B.B., D.M. and V.N.; resources, F.N., I.G.S. and D.V.; data curation, B.B. and D.M.; writing—original draft preparation, C.G.B. and B.B.; writing—review and editing, M.A., I.G.S. and D.V.; visualization, B.B. and C.G.B.; supervision, M.A. and C.G.B.; project administration, C.G.B. and D.M.; funding acquisition, F.N., I.G.S. and D.V. All authors have read and agreed to the published version of the manuscript.

Funding: This research received no external funding.

Data Availability Statement: All data presented in this study were generated by Monte Carlo simulations of the relational network model described in the manuscript. The simulations were performed using custom Python 3.10 scripts executed in Google Colab. No external datasets were used. The simulation code and numerical data supporting the reported results are available from the corresponding author upon reasonable request.

Conflicts of Interest: The authors declare no conflicts of interest.

References

1. Bardeen, J.; Cooper, L.N.; Schrieffer, J.R. Theory of Superconductivity. *Phys. Rev.* **1957**, *108*, 1175–1204. [CrossRef]
2. Tinkham, M. *Introduction to Superconductivity*, 2nd ed.; McGraw-Hill: New York, NY, USA, 1996.
3. Bednorz, J.G.; Müller, K.A. Possible high Tc superconductivity in the Ba–La–Cu–O system. *Z. Phys. B* **1986**, *64*, 189–193. [CrossRef]
4. Lee, P.A.; Nagaosa, N.; Wen, X.-G. Doping a Mott insulator: Physics of high-temperature superconductivity. *Rev. Mod. Phys.* **2006**, *78*, 17–85. [CrossRef]
5. Dagotto, E. Complexity in strongly correlated electronic systems. *Science* **2005**, *309*, 257–262. [CrossRef] [PubMed]
6. Keimer, B.; Kivelson, S.A.; Norman, M.R.; Uchida, S.; Zaanen, J. From quantum matter to high-temperature superconductivity. *Nature* **2015**, *518*, 179–186. [CrossRef] [PubMed]
7. Anderson, P.W. The resonating valence bond state in La_2CuO_4 and superconductivity. *Science* **1987**, *235*, 1196–1198. [CrossRef] [PubMed]
8. Scalapino, D.J. A common thread: The pairing interaction for unconventional superconductors. *Rev. Mod. Phys.* **2012**, *84*, 1383–1417. [CrossRef]
9. Wen, X.-G. *Quantum Field Theory of Many-Body Systems*; Oxford University Press: Oxford, UK, 2004.
10. Sachdev, S. *Quantum Phase Transitions*, 2nd ed.; Cambridge University Press: Cambridge, UK, 2011.
11. Rovelli, C. *Quantum Gravity*; Cambridge University Press: Cambridge, UK, 2004.
12. Ollivier, Y. Ricci curvature of Markov chains on metric spaces. *J. Funct. Anal.* **2009**, *256*, 810–864. [CrossRef]
13. Albert, R.; Barabási, A.-L. Statistical mechanics of complex networks. *Rev. Mod. Phys.* **2002**, *74*, 47–97. [CrossRef]
14. Buzea, C.G.; Nedeff, F.; Mirilă, D.; Nedeff, V.; Rusu, O.; Agop, M.; Vasincu, D. An Axiomatic Relational–Informational Framework for Emergent Geometry and Effective Spacetime. *Axioms* **2026**, *15*, 154. [CrossRef]
15. Kosterlitz, J.M.; Thouless, D.J. Ordering, metastability and phase transitions in two-dimensional systems. *J. Phys. C* **1973**, *6*, 1181–1203. [CrossRef]
16. Nelson, D.R.; Kosterlitz, J.M. Universal jump in the superfluid density of two-dimensional superfluids. *Phys. Rev. Lett.* **1977**, *39*, 1201–1205. [CrossRef]
17. Stanley, H.E. *Introduction to Phase Transitions and Critical Phenomena*; Oxford University Press: Oxford, UK, 1971.
18. Fisher, M.E.; Barber, M.N.; Jasnow, D. Helicity modulus, superfluidity, and scaling in isotropic systems. *Phys. Rev. A* **1973**, *8*, 1111–1124. [CrossRef]
19. Stauffer, D.; Aharony, A. *Introduction to Percolation Theory*, 2nd ed.; Taylor & Francis: London, UK, 1994.
20. Georgii, H.-O. *Gibbs Measures and Phase Transitions*, 2nd ed.; De Gruyter Studies in Mathematics 9; Walter de Gruyter: Berlin, Germany, 2011.
21. Bollobás, B. *Modern Graph Theory*; Graduate Texts in Mathematics 184; Springer: New York, NY, USA, 1998.
22. Lyons, R.; Peres, Y. *Probability on Trees and Networks*; Cambridge University Press: New York, NY, USA, 2016.
23. Woess, W. *Random Walks on Infinite Graphs and Groups*; Cambridge Tracts in Mathematics 138; Cambridge University Press: Cambridge, UK, 2000.

24. Newman, M.E.J. *Networks: An Introduction*; Oxford University Press: Oxford, UK, 2010.
25. Metropolis, N.; Rosenbluth, A.W.; Rosenbluth, M.N.; Teller, A.H.; Teller, E. Equation of state calculations by fast computing machines. *J. Chem. Phys.* **1953**, *21*, 1087–1092. [CrossRef]
26. Landau, D.P.; Binder, K. *A Guide to Monte Carlo Simulations in Statistical Physics*, 4th ed.; Cambridge University Press: Cambridge, UK, 2014.
27. Grimmett, G. *Percolation*, 2nd ed.; Springer: Berlin/Heidelberg, Germany, 1999.
28. Havlin, S.; Ben-Avraham, D. Diffusion in disordered media. *Adv. Phys.* **1987**, *36*, 695–798. [CrossRef]
29. Cardy, J. *Scaling and Renormalization in Statistical Physics*; Cambridge University Press: Cambridge, UK, 1996.

Disclaimer/Publisher's Note: The statements, opinions and data contained in all publications are solely those of the individual author(s) and contributor(s) and not of MDPI and/or the editor(s). MDPI and/or the editor(s) disclaim responsibility for any injury to people or property resulting from any ideas, methods, instructions or products referred to in the content.